PCCP

Implementation of RI-CC2 triplet excitation energies with an application to *trans*-azobenzene

Christof Hättig[a] and Kasper Hald[b]

[a] *Forschungszentrum Karlsruhe, Institute of Nanotechnology, P.O. Box 3640, D-76021 Karlsruhe, Germany*
[b] *Department of Chemistry, University of Aarhus, DK-8000 Aarhus C, Denmark*

Received 27th November 2001, Accepted 4th February 2002
First published as an Advance Article on the web 2nd May 2002

Triplet excitation energies within the approximate coupled cluster singles and doubles model CC2 have been implemented using an explicitly spin coupled basis and the resolution of the identity approximation for two-electron integrals. This approach reduces substantially the requirements for CPU time, disk space and memory, and extends the applicability of CC2 for triplet excited states to molecules that could not be studied before with this method. We report an application to the lowest singlet and triplet vertical excitation energies of *trans*-azobenzene. An accurate *ab initio* geometry optimized at the MP2/cc-pVTZ level is presented, and CC2 calculations in the aug-cc-pVTZ basis set with 874 basis functions are combined with coupled cluster singles and doubles (CCSD) calculations in modest basis sets to obtain the best possible estimates for the vertical excitation energies. The results show that recently reported SOPPA calculations are unreliable. Good agreement with experiment is obtained for the lowest excited singlet state S_1, but for the lowest triplet state T_1 the results indicate a large difference between the vertical excitation energy and the experimentally observed transition.

I. Introduction

In a recent series of publications, Hald *et al.*[1–3] have reported an implementation of coupled cluster singles and doubles (CCSD) and the approximate coupled cluster models CC2[4] and CC3[5] for triplet excitation energies using an explicitly spin coupled basis for the excitation operators and the corresponding projection manifold. Compared to a spin orbital based formulation—which has been standard for triplet excitations—the spin coupled formulation reduced the computational requirements significantly. For closed shell systems, the computational costs for the calculation of triplet excitation energies thus became comparable to those for singlet excitations, for which spin coupled formulations have been used for many years.

In the present article we focus on the approximate coupled cluster singles and doubles model CC2, which is obtained from the CCSD model by truncating the equations for the double excitation amplitudes in second-order perturbation theory.[4] This leads to a coupled cluster model for which the computational costs formally scale as nN^4, where n is the number of correlated electrons and N the size of the basis set. CC2 ground state energies and excitation energies for single excitation dominated transitions are both correct to second order in perturbation theory, while excitation energies for double excitation dominated transitions are only correct to zeroth order. This should be compared with the CCSD method for which the computational costs scale as n^2N^4. CCSD provides ground state energies which are correct through third order in perturbation theory, and excitation energies which are also only correct through second order for single excitation dominated transitions, but correct through first order for double excitation dominated transitions. The CC2 method is thus designed for the calculation of excitation energies of modest accuracy ($\approx$0.3 eV error) for which CCSD calculations with accurate basis sets are not possible. However, in integral-direct implementations as they have been reported in refs. 1–3, which employ conventional four-index electron repulsion integrals, the computational costs for both CC2 and CCSD are dominated to a large extent by the costs for the calculation and the transformation of these integrals, which hampers the application of CC2 to large molecules. Other severe bottlenecks for large-scale CC2 calculations with this approach are huge memory and disk space demands which scale as n^2N^2 since the storage of double excitation amplitudes is required.

Recently, Hättig and Weigend have shown that for CC2 both the CPU time and the storage bottlenecks can be removed if the resolution of the identity (RI) approximation for the electron repulsion integrals is employed. We report here an extension of this work to triplet excitations, where we employ the explicitly spin coupled basis reported in ref. 1 to obtain the most efficient formulation. With the RI approximation the operation count for CC2 calculations can be reduced to $\mathcal{O}(n^2N^2N_{\mathrm{aux}})$, where N_{aux} is the size of the auxiliary basis set for the resolution of the identity, which is $\approx 2.5N$. In practice, this means a reduction by about an order of magnitude or more, depending on the basis set size or the ratio n/N.[6,7] Furthermore, the RI approximation makes it possible to separate the calculation and transformation of electron repulsion integrals from the contraction of these integrals with double excitation amplitudes. This allows the use of a partitioned formulation of CC2 which does not require the storage of double excitation amplitudes or other intermediates of $\mathcal{O}(n^2N^2)$ size on disk and removes the storage bottlenecks.

We apply the RI-CC2 implementation to the lowest vertical singlet and triplet excitation energies in *trans*-azobenzene. Azobenzene is the parent compound of a class of dyes which is of interest in the development of materials for optical data storage.[8–10] In thin films of polymers or oligomers of azobenzene dyes the azobenzene group can be aligned by polarized laser light. The alignment changes the diffraction, and the

DOI: 10.1039/b110847f

This journal is © The Owner Societies 2002

information coded in the aligned molecules can be read by another laser. This storage process exploits a *trans*-to-*cis* and *cis*-to-*trans* isomerization process of the electronically excited azobenzene group which involves the lowest singlet and the lowest triplet states. Anyway, the important information which is needed for the optimization of the storage process is the laser wavelength, *i.e.* the transition energy, required to excite the azobenzene group. In the planar molecule the transition to the lowest singlet excited state S_1 is forbidden for symmetry reasons and the lowest allowed transition is the $\pi \rightarrow \pi^*$ excitation into the S_2 state. Because of the size of azobenzene, previous theoretical investigations have been limited to semiempirical and density functional theory (DFT) calculations and a few *ab initio* studies using second-order Møller–Plesset perturbation theory (MP2), configuration interaction (CI), complete active space self-consistent field (CASSCF) or the second-order polarization propagator approach (SOPPA) with small basis sets insufficient to describe correctly the electronic structure.[10–15]

This paper is organized as follows: In the next section we give a brief review of the equations for the CC2 method formulated in an explicitly spin coupled operator basis, and outline the implementation of the RI-CC2 approach for triplet excitation energies. In Section III.A we report a new *ab initio* geometry for *trans*-azobenzene, optimized at the MP2/cc-pVTZ level. The results obtained for the lowest singlet and triplet excitations of *trans*-azobenzene with RI-CC2 calculations in an accurate aug-cc-pVTZ basis and CCSD calculations in small ANO basis sets are presented in Section III.B. In Section IV we give a short summary of our conclusions.

II. Theory and implementation

Starting from the coupled cluster *ansatz* for single reference states

$$|\mathrm{CC}\rangle = \exp(T)|\mathrm{HF}\rangle \tag{1}$$

we obtain the similarity transformed Schrödinger equation

$$\exp(-T)H|\mathrm{CC}\rangle = E|\mathrm{HF}\rangle \tag{2}$$

where T is the cluster operator, H the Hamiltonian for the system and $|\mathrm{HF}\rangle$ the Hartree–Fock reference state. In the CC2 model, the cluster operator is truncated after double excitations. It is written as

$$T = \sum_{\mu_1} t_{\mu_1}\tau_{\mu_1} + \sum_{\mu_2} t_{\mu_2}\tau_{\mu_2} \tag{3}$$

where μ_1 and μ_2 denote respectively single and double excitations, t_μ are the cluster amplitudes and τ_μ the corresponding excitation operators. The amplitudes are determined from cluster equations which for the CC2 model have been defined in ref. 4 as

$$\Omega_{\mu_1} = \langle \mu_1|\hat{\boldsymbol{H}} + \left[\hat{\boldsymbol{H}}, T_2\right]|\mathrm{HF}\rangle = 0 \tag{4}$$

$$\Omega_{\mu_2} = \langle \mu_2|\hat{\boldsymbol{H}} + [F, T_2]|\mathrm{HF}\rangle = 0 \tag{5}$$

where

$$\begin{aligned}\hat{\boldsymbol{H}} &= \exp(-T_1)H\exp(T_1)\\ &= \sum_{pq}\hat{\boldsymbol{h}}_{pq}E_{pq} + \frac{1}{2}\sum_{pqrs}\left(pq\,\hat{|}\,rs\right)\left(E_{pq}E_{rs} - \delta_{qr}E_{ps}\right)\end{aligned} \tag{6}$$

and F is the usual SCF Fock operator. The energy is given by

$$E = \langle \mathrm{HF}|H|\mathrm{CC}\rangle \tag{7}$$

In the canonical SCF MO basis, eqns. (4) and (5) can be solved explicitly for the double excitation amplitudes:

$$t_{aibj} = \frac{(ai\,\hat{|}\,bj)}{\varepsilon_i - \varepsilon_a + \varepsilon_j - \varepsilon_b} \tag{8}$$

Here and in the following i, j, k, l denote occupied and a, b, c, d unoccupied canonical orbitals. Because of the simple structure of the CC2 double excitation amplitudes, these can be generated "on the fly" and do not need to be stored on disk or in memory.

Excitation energies and the amplitudes describing the excited state are obtained as solutions to the asymmetric eigenvalue problem

$$\boldsymbol{AR} = \omega\boldsymbol{SR} \tag{9}$$

where $\boldsymbol{A}$ is the Jacobian for the vector function Ω_μ and $\boldsymbol{S}$ is the overlap matrix

$$A_{\mu\nu} = \frac{\partial\Omega_\mu}{\partial t_\nu} \tag{10}$$

$$S_{\mu\nu} = \langle\mu|\tau_\nu|\mathrm{HF}\rangle \tag{11}$$

and $\boldsymbol{R}$ is a right eigenvector. With the parameterization employed here for the cluster amplitudes, $\boldsymbol{S}$ is a unit matrix. For the CC2 model the Jacobian is

$$A = \begin{pmatrix} \langle\mu_1|\left[\hat{\boldsymbol{H}}, \tau_{\nu_1}\right] + \left[\left[\hat{\boldsymbol{H}}, \tau\nu_1\right], T_2\right]|\mathrm{HF}\rangle & \langle\mu_1|\left[\hat{\boldsymbol{H}}, \tau_{\nu_2}\right]|\mathrm{HF}\rangle \\ \langle\mu_2|\left[\hat{\boldsymbol{H}}, \tau_{\nu_1}\right]|\mathrm{HF}\rangle & \delta_{\mu_2\nu_2}\varepsilon_{\mu_2} \end{pmatrix} \tag{12}$$

where the doubles–doubles block is diagonal with the elements

$$\varepsilon_{aibj} = \varepsilon_a - \varepsilon_i + \varepsilon_b - \varepsilon_j \tag{13}$$

Explicit formulae for the transformation of a trial vector with singlet[16] and triplet[1] spin symmetry have previously been derived and are summarized in Table 1. Capitalizing the diagonal structure of the doubles–doubles block we partition the CC2 eigenvalue problem as

$$\left[A_{\mu_1\nu_1} - \sum_{\gamma_2}\frac{A_{\mu_1\gamma_2}A_{\gamma_2\nu_1}}{\varepsilon_{\gamma_2} - \omega}\right]R_{\nu_1} = A^{\mathrm{eff}}_{\mu_1\nu_1}(\omega)R_{\nu_1} = \omega R_{\mu_1} \tag{14}$$

$$R_{\mu_2} = -\sum_{\nu_1}\frac{A_{\mu_2\nu_1}R_{\nu_1}}{\varepsilon_{\mu_2} - \omega} \tag{15}$$

where now a non-linear eigenvalue problem only in the space of the single excitations needs to be solved. The double excitation part of the eigenvector R is given as a function of the single excitation part by eqn. (15). In order to apply iterative techniques to solve the eigenvalue problem we need the capability to transform, for a given guess for the eigenvalue ω, a trial vector with the effective matrix $\boldsymbol{A}^{\mathrm{eff}}_{\mu_1\nu_1}(\omega)$ in eqn. (14). Explicit expressions for these transformations for both singlet and triplet excitations are given in Table 1. In the latter table we use for triplet excitations the combination

$$R^{ab}_{ij} = 2\left({}^{(+)}R^{ab}_{ij} + {}^{(-)}R^{ab}_{ij}\right) \tag{16}$$

with the individual parts ${}^{(+)}R$ and ${}^{(-)}R$ of the triplet double excitation vector given by

$${}^{(+)}R^{ab}_{ij} = \frac{1}{2}\frac{(\overline{ai}\,|\,bj) + (\overline{bj}\,|\,ai) - (\overline{aj}\,|\,bi) - (\overline{bi}\,|\,aj)}{\varepsilon_i - \varepsilon_a + \varepsilon_j - \varepsilon_b + \omega} \tag{17}$$

$${}^{(-)}R^{ab}_{ij} = \frac{1}{2}\frac{(\overline{bj}\,|\,ai) - (\overline{ai}\,|\,bj)}{\varepsilon_i - \varepsilon_a + \varepsilon_j - \varepsilon_b + \omega} \tag{18}$$

Table 1 Explicit expressions for singlet and triplet trial vectors transformed with the effective CC2 Jacobian $A^{\mathrm{eff}}(\omega)$ defined in eqn. 14

	$\rho(\omega) = A^{\mathrm{eff}}(\omega)R$	
Term	Singlet	Triplet
ρ^1_{ai}	$+\sum_d E_{ad}R_{di}$	$+\sum_d E_{ad}R_{di}$
ρ^2_{ai}	$-\sum_l R_{al}E_{li}$	$-\sum_l R_{al}E_{li}$
ρ^3_{ai}	$+\sum_{ck}[2(ai\hat{\mid}kc)-(ki\hat{\mid}ac)]R_{ck}$	$+\sum_{ck}[2(ai\hat{\mid}kc)-(ki\hat{\mid}ac)]R_{ck}$
ρ^4_{ai}	$+\sum_{dlc}R^{cd}_{il}(ld\hat{\mid}ac)$	$+\sum_{dlc}R^{cd}_{il}(ld\hat{\mid}ac)$
ρ^5_{ai}	$-\sum_{dlk}R^{ad}_{kl}(ld\hat{\mid}ki)$	$-\sum_{dlk}R^{ad}_{kl}(ld\hat{\mid}ki)$
ρ^6_{ai}	$+\sum_{ck}(R^{ac}_{ik}\hat{F}_{kc}-t^{ac(1)}_{ki}\bar{F}_{kc})$	$+\sum_{ck}(R^{ac}_{ik}\hat{F}_{kc}-t^{ac(3)}_{ki}\bar{F}_{kc})$
	${}^{(1)}\bar{F}_{kc}=\sum_{dl}[2(kc\mid ld)-(kd\mid lc)]R_{dl}$	${}^{(3)}\bar{F}_{kc}=-\sum_{dl}(kd\mid lc)R_{dl}$
	$E_{ab}=\hat{F}_{ab}-\sum_{dkl}(2t^{ad}_{kl}-t^{ad}_{lk})(ld\mid kb)$	
	$E_{ji}=\hat{F}_{ji}-\sum_{cdk}(2t^{cd}_{ik}-t^{cd}_{ki})(kd\mid jc)$	

while in the singlet case the double excitation vector is obtained as

$$R^{ab}_{ij}=\frac{1}{2}\frac{2(\overline{ai}\mid bj)+2(\overline{bj}\mid ai)-(\overline{aj}\mid bi)-(\overline{bi}\mid aj)}{\varepsilon_i-\varepsilon_a+\varepsilon_j-\varepsilon_b+\omega} \tag{19}$$

The modified two-electron MO integrals used in eqns. (17)–(19) are defined through a generalized AO to MO transformation

$$(\overline{ai}\mid bj)=\sum_{\alpha\beta\gamma\delta}\left[\bar{\Lambda}^p_{\alpha a}\Lambda^h_{\beta i}+\Lambda^p_{\alpha a}\bar{\Lambda}^h_{\beta i}\right]\Lambda^p_{\gamma b}\Lambda^h_{\delta j}(\alpha\beta|\gamma\delta) \tag{20}$$

with the transformation matrices $\Lambda^p = C(1-t_1^{\mathrm{T}})$, $\Lambda^h = C(1+t_1)$, $\bar{\Lambda}^p = -CR_1^{\mathrm{T}}$ and $\bar{\Lambda}^h = CR_1$, where C is the canonical orbital coefficient matrix and α, β, γ, δ are atomic orbitals.

The partitioning of the CC2 eigenproblem of itself would not reduce the scaling of the memory and disk space requirements since an efficient "on the fly" calculation of either the doubles amplitudes or the doubles part of the trial vector would require the storage of $\mathcal{O}(n^2N^2)$ integrals where N is the number of basis functions and n is the number of electrons. This bottleneck can be avoided with a resolution of the identity approximation for the two-electron integrals.[17–19] In the RI approximation the products of atomic orbitals appearing in the four-index two-electron integrals are expanded in an auxiliary fitting basis,

$$(\alpha\beta|\gamma\delta)=\sum_{PQ}c_{\alpha\beta,P}\,V_{PQ}\,c_{\gamma\delta,Q} \tag{21}$$

$$V_{PQ}=(P\mid Q) \tag{22}$$

where $c_{\alpha\beta,P}$ are the expansion coefficients and $(P|Q)$ are two-index two-electron integrals in the auxiliary basis set. If the expansion is done employing a Coulomb metric,[19,20] the expansion coefficients are obtained in terms of three-index two-electron integrals $(\alpha\beta|P)$ and the two-index two-electron $(V|P)$ integrals by solving a linear set of equations,

$$c_{\alpha\beta,P}=\sum_P(\alpha\beta\mid P)\,V^{-1}_{PQ} \tag{23}$$

and the four-index two-electron integrals can be expanded as[19–22]

$$(\alpha\beta\mid\gamma\delta)=\sum_{PQ}(\alpha\beta\mid P)\,V^{-1}_{PQ}(Q\mid\gamma\delta) \tag{24}$$

This allows one to perform the AO to MO transformation and some of the contractions with three-index integrals instead of four-index integrals and thereby removes the need to store any four-index integrals. The algorithm for calculating transformations of a triplet trial vector with the effective Jacobian in eqn. (14) is summarized in Fig. 1. Compared with the original implementation[1] in the DALTON program package,[23] which employed conventional four-index two-electron integrals, the present approach reduces disk space and memory requirements to $\mathcal{O}(nNN_{\mathrm{aux}})$ and $\mathcal{O}(mNN_{\mathrm{aux}})$, respectively, where m is the size of the subsets of occupied orbitals I, and $N_{\mathrm{aux}}\approx 2.5N$. I/O scales as $\mathcal{O}(n_I nNN_{\mathrm{aux}})$ where n_I is the number of subsets I. The computationally most demanding operations in terms of CPU time and memory requirements are carried out in steps 3 and 5 of the algorithm in Fig. 1. Step 3 describes

1. Calculate $\Lambda^p_{\alpha p}$, $\Lambda^h_{\alpha p}$, $\bar{\Lambda}^p_{\alpha p}$, $\bar{\Lambda}^h_{\alpha p}$
2. $\rho^{1,2}_{ai} \leftarrow E_{ab}R_{bi} - R_{aj}E_{ji}$
3. Loop I (where I is a subset of active occupied orbitals i)

   calculate $(\alpha\beta|P)$ for all α, β, P and read $\hat{B}^Q_{ki}$ for all $i \in I$

   $\bar{B}^Q_{ai} \leftarrow \Lambda^p_{\alpha a}\bar{\Lambda}^h_{\beta i}(\alpha\beta|P)V^{-\frac{1}{2}}_{PQ} - R_{ak}\hat{B}^Q_{ki}$ for all $i \in I$

   store $\bar{B}^Q_{ai}$ on file

   end loop I
4. Form $\bar{F}_{ia} = -\hat{B}^Q_{ja}\hat{B}^Q_{ib}R_{bj}$
5. Loop I

   read $\hat{B}^Q_{ai}$ and $\bar{B}^Q_{ai}$ for i $\in$ I

   loop j

   – read $\hat{B}^Q_{bj}$, $\bar{B}^Q_{bj}$ and $\hat{B}^Q_{jb}$

   – $(\overline{ai}|bj) \leftarrow \bar{B}^Q_{ai}\hat{B}^Q_{bj}$ and $(\overline{bj}|ai) \leftarrow \hat{B}^Q_{ai}\bar{B}^Q_{bj}$

   – $R^{ab}_{ij} \leftarrow \left\{2(\overline{bj}|ai) - (\overline{aj}|bi) - (\overline{bi}|aj)\right\}/\left\{\epsilon_i - \epsilon_a + \epsilon_j - \epsilon_b + \omega\right\}$

   – $\tilde{Y}^Q_{ia} \leftarrow R^{ab}_{ij}\hat{B}^Q_{jb}$ and $\rho^6_{ai} \leftarrow R^{ab}_{ij}\hat{F}_{jb}$

   – $(a\hat{i}|bj) \leftarrow \hat{B}^Q_{ai}\hat{B}^Q_{bj}$

   – $t^{ab}_{ij} \leftarrow (a\hat{i}|bj)/\{\epsilon_i - \epsilon_a + \epsilon_j - \epsilon_b\}$

   – $\rho^6_{ai} \leftarrow \rho^6_{ai} - \hat{t}^{ba}_{ij}\bar{F}_{jb}$

   end loop j

   store $\tilde{Y}^Q_{ia}$ on file

   end loop I
6. Form $\tilde{\Gamma}^P_{i\beta} = \left\{\tilde{Y}^Q_{ia}\Lambda^h_{\beta a} - \bar{\Lambda}^h_{\beta k}\hat{B}^Q_{ki}\right\}V^{-1/2}_{QP}$
7. Loop Φ (where Φ is a subset of atomic orbitals)

   read $\tilde{\Gamma}^P_{i\beta}$ and calculate $(P|\alpha\beta)$ for $\beta \in \Phi$

   $\rho^{JG}_{\alpha i} \leftarrow \tilde{\Gamma}^P_{i\beta}(P|\alpha\beta)$

   end loop Φ
8. $\rho_{ai} \leftarrow \rho^{1,2}_{ai} + \Lambda^p_{\alpha a}\rho^{JG}_{\alpha i} - \tilde{Y}^Q_{ia}B^Q_{ki} + \rho^6_{ai}$

Fig. 1 Algorithm for the transformation of the triplet spin coupled trial R_{μ_1} with the effective Jacobian $A^{\text{eff}}(\omega)$ defined in eqn. (14). The integral intermediates $\hat{B}^Q_{pq} = \lambda^p_{\alpha p}\lambda^h_{\beta q}(\alpha\beta|P)V^{-1/2}_{PQ}$ and the intermediates E_{ab}, E_{ji} and $\hat{F}_{jb}$ are independent of the trial vector R_{μ_1}. These intermediates are precalculated once and for all after the determination of the ground state amplitudes prior to the solution of the eigenvalue problem. For definitions and notations see Section II and Table 1.

the evaluation of transformed three-index two-electron integrals $\bar{B}^Q_{ai}$. The batch size for the loop over the occupied orbitals i is chosen such that the half-transformed integrals $(\alpha i|P) = \sum_\beta \bar{\Lambda}^h_{\beta i}(\alpha\beta|P)$ can be kept in memory for the complete batch I. The AO three-index integrals are evaluated in a batch loop over shell pairs for α, β. The memory requirements for this step are thus $\mathcal{O}(mNN_{\text{aux}})$. The computationally most expensive steps are the construction of the four-index MO integrals $(\overline{ai}|bj)$ and $(\overline{bj}|ai)$ from the three-index intermediates $\hat{B}^Q_{ai}$ and $\bar{B}^Q_{ai}$ and the calculation of the $\tilde{Y}^Q_{ia}$ intermediate—described at step 5—which both take $\mathcal{O}(n^2N^2N_{\text{aux}})$ operations. In these steps, there are no differences in the operation count for triplet and singlet excitations. The differences caused by the different spin couplings appear only in operations scaling as $\mathcal{O}(n^2N^2)$ or less. The computational requirements are thus practically the same for singlet and triplet excitations.

III. *trans*-Azobenzene

A. Structure

The structure of *trans*-azobenzene has been studied experimentally with various spectroscopic methods in the solid, the liquid, and the gas phase, but it is still a matter of dispute. The first X-ray diffraction results[24,25] suggested that the *trans*-azobenzene (TAB) molecule has a planar structure with C_{2h} symmetry in the solid phase. A recent reinvestigation,[26] however, showed that there are two crystallographically independent sites in the crystal and that the symmetry group of the TAB molecule in the crystal is only C_i. Early gas electron diffraction (GED) measurements,[27] on the other hand, indicated that in the gas phase the geometry is slightly distorted from planarity to a structure with C_i symmetry and also for the liquid phase a distorted geometry with C_i molecular symmetry is found in Raman experiments.[28] A very recent accurate GED measurement by Tsuji *et al.*,[29] however, led to the conclusion that the gas phase equilibrium structure has indeed C_{2h} symmetry. Theoretically the structure has been studied at the Hartree–Fock and the density functional theory (DFT) level with different functionals using the 6-31G* basis. Also second-order Møller–Plesset perturbation theory (MP2) has been used,[11,29] but only in combination with small basis sets insufficient for a description of electron correlation effects.

We have therefore performed a new geometry optimization at the MP2 level using the cc-pVTZ basis set of Dunning and coworkers.[30] In these calculations we imposed C_{2h} molecular symmetry, *i.e.* a planar geometry, as found in the latest GED experiment for the gas phase structure. Anyway, after distorting the molecule into C_i or into C_2 symmetry, optimizations resulted again in essentially planar geometries. For these calculations we employed the DSCF[31] and RI-MP2[22] modules of the TURBOMOLE program package.[32] In the MP2 calculations the $1s^2$ shells of the carbon and nitrogen atoms were kept frozen and for the resolution of the identity approximation in the RI-MP2 program the optimized auxiliary cc-pVTZ basis from ref. 7 was used. The details of the structure are given in Table 2, together with the experimental data from refs. 25 and 27 and the B3LYP/6-31G* results from ref. 12. The atom numbering is explained in Fig. 2.

Comparing the MP2/cc-pVTZ results with the previous DFT results in the 6-31G* basis, it is observed that the differences for the angles and the bond lengths are small compared with the experimental uncertainties. The largest differences are observed for the N=N bond lengths and the C(3)–N(1)=N(2) angle. The deviations between the B3LYP and B3P86 and the present MP2 results are within $\|\delta r\| \approx 4$ mÅ and an average change of 0.2° in the angles, the smallest within the five DFT functionals used in ref. 12. For the three other functionals—SVWN, BLYP and BP86—the average differences in the bond lengths are 9, 13 and 12 mÅ respectively. The angles for SVWN deviate on average by 0.6° from the MP2 results, whereas the differences are only 0.3° and 0.2° for BLYP and BP86. The largest deviations are found for the angles C(3)–N(1)=N(2), C(5)–C(3)–C(7) and C(15)–C(5)–C(3). Anyway, the present MP2/cc-pVTZ geometry is expected to be the most accurate *ab initio* structure available for *trans*-azobenzene and should be useful for a refinement of the GED structures, which rely on *ab initio* data for a full determination of all structure parameters, and the latest analysis[29] was based on an MP2/6-31+G* calculation.

B. Vertical excitation energies

The vertical excitation energies of *trans*-azobenzene were calculated using the RI-CC2 approach described above, the usual CC2 (without RI approximation) and the CCSD methods. For all models the $1s^2$ cores at the nitrogen and carbon atoms were kept frozen in the correlation and response calculations. In the CC2 and CCSD calculations we employed the same contractions of the atomic natural orbital (ANO) basis sets by Widmark *et al.*[33] that have been used in the SOPPA calculations by Åstrand *et al.*[10] The first one—denoted as [3s2p1d/2s]—was taken from the work of Molina *et al.*[34,35] and consists of two contracted functions for hydrogen and a [3s2p1d] contraction for carbon and nitrogen. A second smaller ANO contrac-

Table 2 The MP2/cc-pVTZ optimized geometry of *trans*-azobenzene. A planar geometry with C_{2h} symmetry was enforced. For technical details see Section III.A

	Ab initio calculations		Experiments			
Bond	MP2/cc-pVTZ	B3LYP/6-31G*[a]	X-ray[b]	X-ray[c]	GED[d]	GED[e]
Bond length/Å						
N(2)=N(1)	1.268	1.260	1.257	1.247	1.268	1.260(8)
C(3)–N(1)	1.417	1.418	1.437	1.428	1.427	1.427(8)
C(5)–C(3)	1.400	1.405	1.385	1.389	1.396	1.405
C(7)–C(3)	1.397	1.401	1.385	1.387	1.396	1.401
C(9)–C(7)	1.391	1.393	1.385	1.384	1.396	1.396
C(11)–C(9)	1.393	1.395	1.385	1.382	1.396	1.397
C(13)–C(11)	1.398	1.401	1.385	1.391	1.396	1.402
C(13)–C(5)	1.388	1.389	1.385	1.384	1.396	1.393
H(15)–C(5)	1.080	1.084	1.084		1.088	1.102(7)
H(17)–C(7)	1.081	1.085	1.084		1.088	1.102(7)
H(19)–C(9)	1.081	1.086	1.084		1.088	1.102(7)
H(21)–C(11)	1.081	1.086	1.084		1.088	1.102(7)
H(23)–C(13)	1.082	1.086	1.084		1.088	1.102(7)
Angles/degree						
C(3)–N(1)=N(2)	113.7	114.7	113.0	114.1	114.5	113.6(8)
C(5)–C(3)–N(1)	124.6	124.7		123.7	123.0	124.7(9)
C(7)–C(3)–N(1)	115.1	115.3		115.6		
C(3)–C(5)–C(13)	119.3	119.5		119.1		
C(3)–C(7)–C(9)	120.1	120.2		119.6		
C(5)–C(13)–C(11)	120.5	120.4		120.5		
C(5)–C(3)–C(7)	120.3	119.8		120.7		
C(13)–C(11)–C(9)	120.0	120.0		119.7		
C(11)–C(9)–C(7)	119.8	119.7		120.3		
H(15)–C(5)–C(3)	119.1	118.6				
H(15)–C(5)–C(13)	121.6	121.7				
H(23)–C(13)–C(5)	119.7	119.7				
H(23)–C(13)–C(11)	119.8	119.8				
H(21)–C(11)–C(13)	119.9	119.9				
H(21)–C(11)–C(9)	120.0	120.0				
H(19)–C(9)–C(11)	120.2	120.1				
H(19)–C(9)–C(7)	120.0	120.0				
H(17)–C(7)–C(9)	121.6	121.6				
H(17)–C(7)–C(3)	118.3	118.1				

[a] Density functional theory, ref. 12. [b] X-ray diffraction, ref. 24; for the SOPPA calculations in ref. 10 and the present CCSD calculations for this structure, the angles C–C–C, C–C–N and C–C–H were assumed to be 120°. [c] X-ray diffraction, ref. 25. [d] Gas electron diffraction, ref. 27. [e] Gas electron diffraction, ref. 29; in addition to values given in the table, also the angle difference [C(5)–C(3)–N(1) − C(7)–C(3)–N(1)]/2 was determined to be 5.0(9).

tion—denoted as [3s2p(1d)/2s]—is obtained by leaving out the d-type polarization functions at the carbon atoms, including them only for the nitrogen atoms in the azo group. For the RI-CC2 calculations we employed the aug-cc-pVDZ and aug-cc-pVTZ basis sets of Dunning and coworkers,[30,36] and for the resolution of the identity approximation the optimized aug-cc-pVDZ and aug-cc-pVTZ auxiliary basis sets of Weigend *et al.*[7] To test whether, in the investigated range of the spectrum, some states have (partial) Rydberg character, we performed in addition a RI-CC2 calculation in an aug-cc-pVDZ basis augmented with two primitive (2s2p2d) sets of diffuse functions (exponents 0.01 and 0.0033, as proposed in ref. 16 for a benzene molecule), located at the center of mass of each of the two C_6 rings in *trans*-azobenzene. We denote this basis in the following as aug-cc-pVDZ-CM2. As shown in ref. 7, the aug-cc-pVTZ basis gives at the MP2 level (valence) correlation energies within $\approx 11 \pm 2\%$ of the basis set limit and (valence) correlation contributions to dipole moments within $\approx 7 \pm 6\%$ of the basis set limit, while the additional error introduced by the resolution of the identity approximation is about an order of magnitude smaller. A similar accuracy is expected for CC2 ground state and excitation energies.

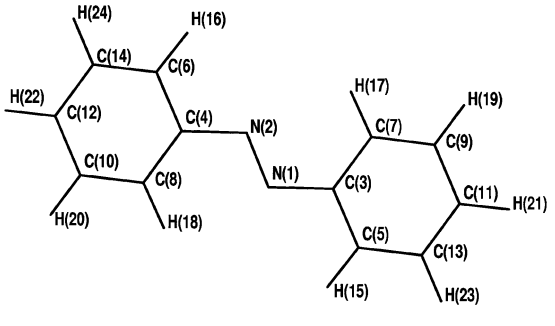


Fig. 2 Geometry and atom numbering for *trans*-azobenzene.

In Table 3 we have listed the lowest singlet and triplet excitation energies computed with the CCSD model and the [3s2p1d/2s] basis and the SOPPA results from ref. 10 obtained in the same basis set. We have calculated the CCSD excitation energies using both the planar X-ray diffraction structure from ref. 24 which was used in the SOPPA calculations by Åstrand *et al.*[10] and the MP2/cc-pVTZ optimized geometry. The two geometries differ mainly in the parameters that describe the azo group, *i.e.* the N=N and C–N bond lengths and the C–N–N angle. Focusing first on the CCSD results for the two different structures, we observe large changes in the vertical

Table 3 Singlet and triplet excitation energies using the [3s2p1d/2s] basis set

State	SOPPA[a]	CCSD[a]	CCSD[b]	$\%T_1$(CCSD[b])
Singlet				
$1\ ^1B_g$	2.31	2.94	3.06	93.6
$1\ ^1B_u$	3.71	3.85	4.46	93.0
$2\ ^1B_u$	4.07	4.31	4.71	91.0
$1\ ^1A_g$	4.08	4.33	4.69	90.4
$2\ ^1A_g$	4.83	5.05	5.64	91.9
$2\ ^1B_g$	5.50	6.90	6.59	90.5
$3\ ^1B_u$	5.53	5.85	6.27	92.0
$3\ ^1A_g$	5.57	5.88	6.30	91.6
$1\ ^1A_u$	5.58	5.71	6.65	90.7
$2\ ^1A_u$	5.77	6.81	6.75	90.2
Triplet				
$1\ ^3B_g$	1.57	2.21	2.36	98.3
$1\ ^3B_u$	2.40	1.75	2.65	98.3
$1\ ^3A_g$	3.55	3.62	3.80	98.6
$2\ ^3B_u$	3.85	4.03	4.34	97.9

[a] Results at the X-ray diffraction geometry from ref. 24. [b] Results at the MP2/cc-pVTZ optimized equilibrium geometry.

excitation energies between the two geometries. Only for the $1\ ^1B_g$, $2\ ^1A_u$, $1\ ^3B_g$ and $1\ ^3A_g$ states the changes are less than 0.2 eV. For all other states we find changes between 0.3 and 1.0 eV. Two conclusions can be drawn from these results: first, for some of the states the vertical excitation energies are probably so sensitive to geometry effects that only limited comparison will be possible with experimental data; and second, the crystal structure from ref. 24 is probably too inaccurate to be appropriate for use in *ab initio* calculations. Before comparing the CCSD and the SOPPA results, we note that in SOPPA, similarly as in the CC2 model, excitation energies are correct through second-order perturbation theory for single excitation dominated transitions, but only correct through zeroth order for double excitations. Since CCSD treats doubles excitations correctly through first order, it provides a benchmark for both SOPPA and CC2.[4,37] If one compares the SOPPA results from ref. 10 with CCSD excitation energies calculated at the same geometry and with the same basis sets, differences larger than 0.6 eV are found for the lowest excited states $1\ ^1B_g$, $1\ ^3B_g$ and $1\ ^3B_u$. This indicates that these states are not correctly described by SOPPA.

In Table 4 we have listed the CC2 excitation energies for the [3s2p(1d)/2s] and the [3s2p1d/2s] basis sets as well as the RI-CC2 results for the aug-cc-pVTZ basis. It has been demonstrated that the RI approximation for CC2 excitation energies only gives rise to errors of the order of meV,[6] meaning that the differences between the results in Table 4 are solely caused by differences in the one-electron basis sets. It is not surprising that there are significant changes in the excitation energies between the [3s2p(1d)/2s] and the [3s2p1d/1s] basis sets for the higher lying states, because the polarization functions at the carbon atoms—excluded in the [3s2(1d)/2s] basis—are necessary for a quantitative description of the two phenyl rings. Nevertheless, the changes are moderate for the lowest excitations, since these are dominated by transitions at the azo group. Going from the [3s2p1d/2s] to the aug-cc-pVTZ basis the CC2 results for all states investigated here change only little. For the singlet states we obtain shifts of 0.07–0.19 eV, whereas the triplet excitation energies change only by 0.01–0.05 eV. We therefore expect that the CC2 results in the aug-cc-pVTZ basis are practically converged with respect to the one-electron basis. This is corroborated by the results obtained in the aug-cc-pVDZ and aug-cc-pVDZ-CM2 basis sets. These two basis sets gave CC2 vertical excitation energies which deviated by less than 0.02 eV between aug-cc-pVDZ and aug-cc-pVDZ-CM2 and by less than 0.05 eV from the aug-cc-pVTZ results for all investigated states, with the exception of $3\ ^1A_g$ and $2\ ^1A_u$. For the latter states the aug-cc-VDZ results are 5.73 eV ($3\ ^1A_g$) and 5.93 eV ($2\ ^1A_u$) and the aug-cc-pVDZ-CM2 basis gave 5.64 eV ($3\ ^1A_g$) and 5.85 eV ($2\ ^1A_u$). This shows that, with the exception of the latter two states, all the investigated states have pure valence character and that the aug-cc-pVTZ results must be close to the CC2 basis set limit.

The basis set dependence increases with the correlation level, *i.e.* at the CCSD level the basis set effects are slightly larger than for SOPPA and CC2. In Table 5 we have summarized the CC2 and CCSD excitation energies in the [3s2p1d/2s] basis and the RI-CC2 results in the aug-cc-pVTZ basis set. Though the basis set effects are slightly larger for CCSD than for CC2, we correct the CCSD result obtained in the [3s2p1d] basis for the remaining basis set effect by the difference between the two CC2 results to obtain best estimates for the excitation energies. The results are denoted in Table 5 as "extrapolated CCSD" excitation energies. For the lowest singlet excited state $1\ ^1B_g$ we obtain very good agreement with the experimental results for the band maxima. The agreement is less favourable for the $1\ ^1B_u$ and $3\ ^1B_u$ states, but still acceptable, taking into account that we compare calculated electronic vertical excitation energies, not corrected for vibrational effects, with the experimentally observed band maxima. For the triplet states, the comparison of the extrapolated CCSD energies with the

Table 4 CC2 singlet and triplet excitation energies using the MP2/cc-pVTZ geometry

State	CC2/[3s2p(1d)/2s]	CC2/[3s2p1d/2s]	RI-CC2/aug-pVDZ	RI-CC2/aug-pVDZ-CM2	RI-CC2/aug-pVTZ	$\%T_1$(RI-CC2)
Singlet						
$1\ ^1B_g$	3.09	2.94	2.89	2.89	2.84	93.9
$1\ ^1B_u$	4.31	4.14	4.07	4.07	4.04	91.8
$2\ ^1B_u$	4.66	4.51	4.48	4.48	4.44	90.5
$1\ ^1A_g$	4.67	4.52	4.49	4.49	4.45	90.5
$2\ ^1A_g$	5.48	5.26	5.19	5.18	5.15	90.9
$2\ ^1B_g$	6.30	5.83	5.65	5.65	5.64	90.0
$3\ ^1B_u$	6.19	5.93	5.81	5.81	5.79	91.5
$3\ ^1A_g$	6.22	5.96	5.73	5.64	5.80	91.5
$1\ ^1A_u$	6.41	5.94	5.79	5.79	5.78	89.9
$2\ ^1A_u$	6.56	6.15	5.93	5.85	5.97	90.6
Triplet						
$1\ ^3B_g$	2.41	2.30	2.27	2.27	2.26	98.1
$1\ ^3B_u$	2.89	2.84	2.83	2.83	2.83	98.0
$1\ ^3A_g$	4.08	4.04	4.04	4.04	4.03	98.2
$2\ ^3B_u$	4.50	4.29	4.27	4.27	4.24	97.3

Table 5 Summary of the CC2 and CCSD results for the vertical excitation energies at the MP2/cc-pVTZ geometry in comparison with the available experimental data. For RI-CC2 the oscillator strengths in length gauge are given in parentheses

State	Type	CC2/[3s2p1d/2s]	CCSD/[3s2p1d/2s]	RI-CC2/aug-cc-pVTZ	CCSD extrapolated	Experiment
Singlet						
$1\ ^1B_g$	$n \rightarrow \pi^*$	2.94	3.06	2.84	2.95	2.95[a], 2.78–2.82[b]
$1\ ^1B_u$	$\pi \rightarrow \pi^*$	4.14	4.46	4.04 (0.85)	4.36	3.86[a], 3.86–3.95[b]
$2\ ^1B_u$	$\pi_2 \rightarrow \pi^*$	4.51	4.70	4.44 (0.02)	4.63	
$1\ ^1A_g$	$\pi_3 \rightarrow \pi^*$	4.52	4.69	4.45	4.62	
$2\ ^1A_g$	$\pi_4 \rightarrow \pi^*$	5.26	5.64	5.15	5.53	
$2\ ^1B_g$	$n \rightarrow \pi_2^*$	5.83	6.59	5.64	6.40	
$3\ ^1B_u$	$\pi \rightarrow \pi_2^*$	5.93	6.27	5.79 (0.35)	6.13	5.41[a], 5.38–5.51[b]
$3\ ^1A_g$	$\pi \rightarrow \pi_3^*$	5.96	6.30	5.80	6.14	
$1\ ^1A_u$	$\sigma \rightarrow \sigma^*$	5.94	6.65	5.78 (0.00)	6.49	
$2\ ^1A_u$	$\sigma \rightarrow \sigma_2^*$	6.15	6.75	5.97 (0.00)	6.57	
Triplet						
$1\ ^3B_g$	$n \rightarrow \pi^*$	2.30	2.36	2.26	2.31	1.57[c]
$1\ ^3B_u$	$\pi \rightarrow \pi^*$	2.84	2.65	2.83	2.64	2.0–2.1[d]
$1\ ^3A_g$	$\pi_3 \rightarrow \pi^*$	4.04	3.80	4.03	3.79	
$2\ ^3B_u$	$\pi_3 \rightarrow \pi^*$	4.29	4.34	4.24	4.29	

[a] Ref. 38. [b] Ranges of values from λ_{max} in the absorption spectra reported in refs. 39–44. [c] From flash kinetic spectrophotometry, ref. 45. [d] From a magnetic optical rotation dispersion (MORD) spectrum for isomeric azobenzene, ref. 46.

experimental results reveals a huge difference of 0.74 eV for the lowest triplet state $1\ ^3B_g$, which can hardly be explained by remaining basis set or higher-order correlation effects. For this state the basis set effects have been small in the series [3s2p(1d)/2s]–[3s2p1d/2s]–aug-cc-pVTZ, and also the change from CC2 to CCSD is (at $\approx$0.06 eV) relatively small. We therefore conclude that the observed difference of 0.74 eV must be due to a geometry effect, *i.e.* that the excited state equilibrium geometry for this state differs significantly from the ground state geometry and that the observed transition cannot be compared with the calculated vertical excitation energy. While the excitation energies for the singlet states and for the second-lowest triplet state are from absorption and magnetic optical rotation dispersion spectra for the ground state, the excitation energy for the lowest excited triplet state was extracted from the results of a flash kinetic spectrophotometry study with different sensitizers. The determined transition energy thus corresponds rather to an emission from the excited triplet state than to an absorption from the ground state equilibrium.

IV. Conclusions

An implementation of triplet excitation energies within the CC2 model has been described which employs the resolution of identity (RI) approximation for two-electron integrals. The RI approximation leads to a large reduction in the operation count and allows the use of a partitioned form of the CC2 eigenvalue problem, where doubles amplitudes are calculated "on the fly" and do not need to be stored in memory or on disk. Memory and disk space requirements are thereby reduced to $\mathcal{O}(N^2)$ and $\mathcal{O}(N^3)$, respectively. An application to the lowest excited states of *trans*-azobenzene is represented, where RI-CC2 calculations for the aug-cc-pVTZ basis (874 functions) are combined with CCSD calculations in a smaller basis to obtain the best possible estimates for the electronic vertical excitation energies. For these calculations we have employed a geometry optimized at the MP2/cc-pVTZ level, which should be the most accurate *ab initio* structure available for *trans*-azobenzene. The convergence of the CC2 vertical excitation energies with respect to the cardinal number (ζ-level) of the one-electron basis and with respect to diffuse Rydberg functions was tested by calculations in the aug-cc-pVDZ basis and an aug-cc-pVDZ basis augmented with diffuse Rydberg functions. All investigated excited states, with the exception of $3\ ^1A_g$ and $2\ ^1A_u$, are found to have pure valence character, and the basis set effects when going from the aug-cc-pVDZ to the aug-cc-VTZ basis are found to be small compared to other remaining error sources.

The present results suggest that previous SOPPA calculations in a non-optimized geometry are inaccurate for most excited states. With the present calculations, good agreement with the available experimental data is obtained for the lowest excited singlet state. For the lowest triplet state a large difference between the calculated electronic vertical excitation energy and the experimentally observed transition is found. This difference can probably be attributed mostly to a difference between the ground state and the excited state equilibrium geometries.

The main sources of errors in the extrapolated CCSD results are the neglect of vibrational effects, *i.e.* the comparison of electronic vertical excitation energies with the observed band maxima. Furthermore there seems to be a large geometry effect for the excitation energies. In order to obtain more information about the system one would need to determine the equilibrium geometry of the excited states. For systems of the size of *trans*-azobenzene, geometry optimizations for excited states are, however, not feasible at a correlated level with the programs available today. Compared to the effects mentioned above, the errors due to the neglect of higher-order contributions to the coupled cluster expansion and remaining basis errors are expected to be small.

Acknowledgement

This work was supported by the Danish Research Council (Grant No. 9901973).

References

1 K. Hald, D. Yeager, C. Hättig and P. Jørgensen, *Chem. Phys. Lett.*, 2000, **328**, 291.
2 K. Hald, C. Hättig and P. Jørgensen, *J. Chem. Phys.*, 2000, **113**, 7765.
3 K. Hald, C. Hättig, J. Olsen and P. Jørgensen, *J. Chem. Phys.*, 2001, **115**, 3545.
4 O. Christiansen, H. Koch and P. Jørgensen, *Chem. Phys. Lett.*, 1995, **243**, 409.

5 H. Koch, O. Christiansen, P. Jørgensen, A. S. de Merás and T. Helgaker, *J. Chem. Phys.*, 1997, **106**, 1808.
6 C. Hättig and F. Weigend, *J. Chem. Phys.*, 2000, **113**, 5154.
7 F. Weigend, A. Köhn and C. Hättig, *J. Chem. Phys.*, 2002, **116**, 3175.
8 R. Hildebrandt, M. Hegelich, H.-M. Keller, G. Marowsky, S. Hvilsted, N. C. R. Holme and P. S. Ramanujam, *Phys. Rev. Lett.*, 1998, **81**, 5548.
9 P. H. Rasmussen, P. S. Ramanujam, S. Hvilsted and R. H. Berg, *J. Am. Chem. Soc.*, 1999, **121**, 4738.
10 P.-O. Åstrand, P. S. Ramanujam, S. Hvilsted, K. L. Bak and S. P. A. Sauer, *J. Am. Chem. Soc.*, 2000, **122**, 3482.
11 D. R. Armstrong, J. Clarkson and W. E. Smith, *J. Phys. Chem.*, 1995, **99**, 17 825.
12 N. Biswas and S. Umapathy, *J. Phys. Chem. A*, 1997, **101**, 5555.
13 S. Monti, G. Orlandi and P. Palmieri, *Chem. Phys.*, 1982, **71**, 87.
14 P. Cattaneo and M. Persico, *Phys. Chem. Chem. Phys.*, 1999, **1**, 4739.
15 T. Ishikawa, T. Noro and T. Shoda, *J. Chem. Phys.*, 2001, **115**, 7503.
16 O. Christiansen, H. Koch, P. Jørgensen and T. Helgaker, *Chem. Phys. Lett.*, 1996, **263**, 530.
17 J. L. Whitten, *J. Chem. Phys.*, 1973, **58**, 4496.
18 B. I. Dunlap, J. W. D. Connolly and J. R. Sabin, *J. Chem. Phys.*, 1979, **71**, 3396.
19 O. Vahtras, J. E. Almlöf and M. W. Feyereisen, *Chem. Phys. Lett.*, 1993, **213**, 514.
20 M. W. Feyereisen, G. Fitzgerald and A. Komornicki, *Chem. Phys. Lett.*, 1993, **208**, 359.
21 D. E. Bernholdt and R. J. Harrison, *Chem. Phys. Lett.*, 1996, **250**, 477.
22 F. Weigend and M. Häser, *Theor. Chim. Acc.*, 1997, **97**, 331.
23 T. Helgaker, H. J. Å. Jensen, P. Jørgensen, J. Olsen, K. Ruud, H. Ågren, A. A. Auer, K. L. Bak, V. Bakken, O. Christiansen, S. Coriani, P. Dahle, E. K. Dalskov, T. Enevoldsen, B. Fernandez, C. Hättig, K. Hald, A. Halkier, H. Heiberg, H. Hettema, D. Jonsson, S. Kirpekar, R. Kobayashi, H. Koch, K. V. Mikkelsen, P. Norman, M. J. Packer, T. B. Pedersen, T. A. Ruden, A. Sanchez, T. Saue, S. P. A. Sauer, B. Schimmelpfennig, K. O. Sylvester-Hvid, P. R. Taylor and O. Vahtras, *Dalton–an electronic structure program*, Release 1.2, 2001.
24 C. J. Brown, *Acta Crystallogr.*, 1966, **21**, 146.
25 J. A. Bouwstra, A. Schouten and J. Kroon, *Acta Crystallogr. C*, 1983, **39**, 1121.
26 J. Harada, K. Ogawa and S. Tomoda, *Acta Crystallogr. B*, 1997, **53**, 662.
27 M. Traetteberg, I. Hilmo and K. Hagen, *J. Mol. Struct.*, 1977, **39**, 231.
28 B. Kellerer, H. H. Hacker and J. Brandmüller, *Ind. J. Pure Appl. Phys.*, 1971, **9**, 903.
29 T. Tsuji, H. Takashima, H. Takeuchi, T. Egawa and S. Konaka, *J. Phys. Chem. A*, 2001, **105**, 9347.
30 T. H. Dunning, *J. Chem. Phys.*, 1989, **90**, 1007.
31 M. Häser and R. Ahlrichs, *J. Comput. Chem.*, 1989, **10**, 104.
32 R. Ahlrichs, M. Bär, M. Häser, H. Horn and C. Kölmel, *Chem. Phys. Lett.*, 1989, **162**, 165.
33 P.-O. Widmark, B. J. Persson and B. O. Roos, *Theor. Chim. Acta*, 1991, **79**, 419.
34 V. Molina, M. Merchán and B. O. Roos, *J. Phys. Chem. A*, 1997, **101**, 3478.
35 V. Molina, M. Merchán and B. O. Roos, *Spectrochim. Acta A*, 1999, **55**, 433.
36 R. A. Kendall, T. H. Dunning and R. J. Harrison, *J. Chem. Phys.*, 1992, **96**, 6796.
37 O. Christiansen, PhD Thesis, University of Aarhus, 1997.
38 H. H. Jaffé, S.-J. Yeh and R. W. Gardner, *J. Mol. Spectrosc.*, 1958, **2**, 120.
39 H. Rau, in *Photochromism, Molecules and Systems*, ed. H. Dürr and H. Bouas-Laurent, Elsevier, Amsterdam, 1990, vol. 1, ch. 4, pp. 165–192.
40 J. Griffiths, *Chem. Soc. Rev.*, 1972, **1**, 481.
41 I. K. Lednev, T.-Q. Ye, R. E. Hester and J. N. Moore, *J. Phys. Chem.*, 1996, **100**, 13 338.
42 I. K. Lednev, T.-Q. Ye, P. Matousek, M. Townie, P. Foggi, F. V. R. Neuwahl, S. Umapathy, R. E. Hester and J. N. Moore, *Chem. Phys. Lett.*, 1998, **290**, 68.
43 T. Nägele, R. Hoche, W. Zinth and J. Wachtveitl, *Chem. Phys. Lett.*, 1997, **272**, 489.
44 P. Hamm, S. M. Ohline and W. Zinth, *J. Chem. Phys.*, 1997, **106**, 519.
45 S. Monti, E. Gardini, P. Bortolius and E. Amouyal, *Chem. Phys. Lett.*, 1981, **77**, 115.
46 V. E. Shashoua, *J. Am. Chem. Soc.*, 1960, **82**, 5505.